ACS APPLIED MATERIALS & INTERFACES

Letter

www.acsami.org

Culturing Primary Human Osteoblasts on Electrospun Poly(lactic-co-glycolic acid) and Poly(lactic-co-glycolic acid)/Nanohydroxyapatite Scaffolds for Bone Tissue Engineering

Mengmeng Li,[†,‡,§] Wenwen Liu,[†,§] Jiashu Sun,*[,†] Yunlei Xianyu,[†] Jidong Wang,[†] Wei Zhang,[†] Wenfu Zheng,[†] Deyong Huang,[⊥] Shiyu Di,[†] Yun-Ze Long,*[,‡] and Xingyu Jiang*[,†]

[†]National Center for NanoScience & Technology, Beijing 100190, P. R. China

[‡]College of Physics, State Key Laboratory Cultivation Base of New Fiber Materials and Modern Textile, Qingdao University, Qingdao 266071, P. R. China

[⊥]JiShuiTan Hospital, Beijing 100035, P. R. China

Supporting Information

ABSTRACT: In this work, we fabricated polymeric fibrous scaffolds for bone tissue engineering using primary human osteoblasts (HOB) as the model cell. By employing one simple approach, electrospinning, we produced poly(lactic-co-glycolic acid) (PLGA) scaffolds with different topographies including microspheres, beaded fibers, and uniform fibers, as well as the PLGA/nanohydroxyapatite (nano-HA) composite scaffold. The bone-bonding ability of electrospun scaffolds was investigated by using simulated body fluid (SBF) solution, and the nano-HA in PLGA/nano-HA composite scaffold can significantly enhance the formation of the bonelike apatites. Furthermore, we carried out in vitro experiments to test the performance of electrospun scaffolds by utilizing both mouse preosteoblast cell line (MC 3T3 E1) and HOB. Results including cell viability, alkaline phosphatase (ALP) activity, and osteocalcin concentration demonstrated that the PLGA/nano-HA fibers can promote the proliferation of HOB efficiently, indicating that it is a promising scaffold for human bone repair.

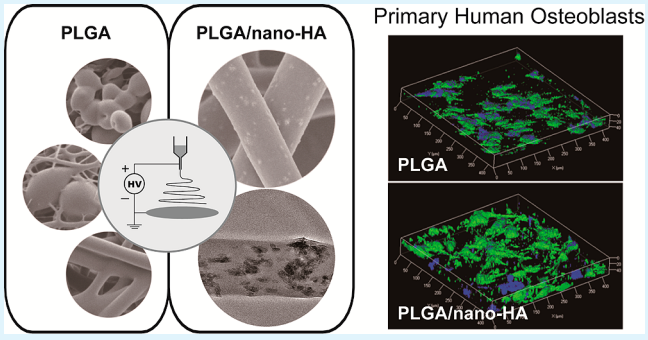

KEYWORDS: *electrospinning, microstructure, hydroxyapatite, human bone repair, biodegradable scaffold*

INTRODUCTION

This report presents electrospun poly(lactic-co-glycolic acid) (PLGA) scaffolds with varying microscale morphologies and embedded nanoscale hydroxyapatite (nano-HA) for bone tissue engineering using primary human osteoblasts as the model cell. An ideal synthetic bone substitute for human bone repair should mimic the physiological and mechanical characteristics of the bone, which has complex composition and multiple functions, such as supporting muscular contraction and protecting the internal organs.[1,2] An important example of the bone substitute is the porous/fibrous scaffold with properties similar to the bone extracellular matrix (ECM), serving as a platform for cell attachment, survival, proliferation, and differentiation.[3] Moreover, the deposited materials inside the scaffold, such as collagen, gelatin, chitosan, and hyaluronic acid, are important for promoting bone tissue regeneration, increasing biocompatibility, and improving the mechanical properties of artificial scaffolds.[4,5]

Current treatments for bone reconstruction are cumbersome and expensive but still yield poor healing because of the lack of appropriate scaffolds and reliable cell sources.[6] Artificial biomaterial scaffolds, especially fibrous scaffolds that support cell and tissue growth, are in high demand. In recent years, many research groups have reported a variety of techniques, such as electrospinning (ES), self-assembly, phase separation, bacterial cellulose, templating, drawing, extraction, vapor-phase polymerization, and kinetically controlled solution synthesis, to fabricate micro/nanoscale fibrous scaffolds.[7−12] Among these approaches, ES is unique and provides particularly attractive advantages, including simple protocols, low cost, high production rate, large surface area-to-volume ratio, and wide choice of materials.[13] The conventional ES setup only requires a high-voltage power supply, a syringe with a metal needle, and a conductive collector, as shown in Figure 1a. The anode of the supply is connected with the needle, and the cathode with the collector. When the electrostatic force generated by the applied high voltage exceeds the surface tension of the polymer droplet in needle point, a charged jet is formed and accelerated toward the grounded collector. As the solvent evaporates, the superfine fibers are deposited with random orientation, known as the

Received: May 21, 2013
Accepted: June 22, 2013
Published: June 22, 2013

   dx.doi.org/10.1021/am401937m | ACS Appl. Mater. Interfaces 2013, 5, 5921−5926

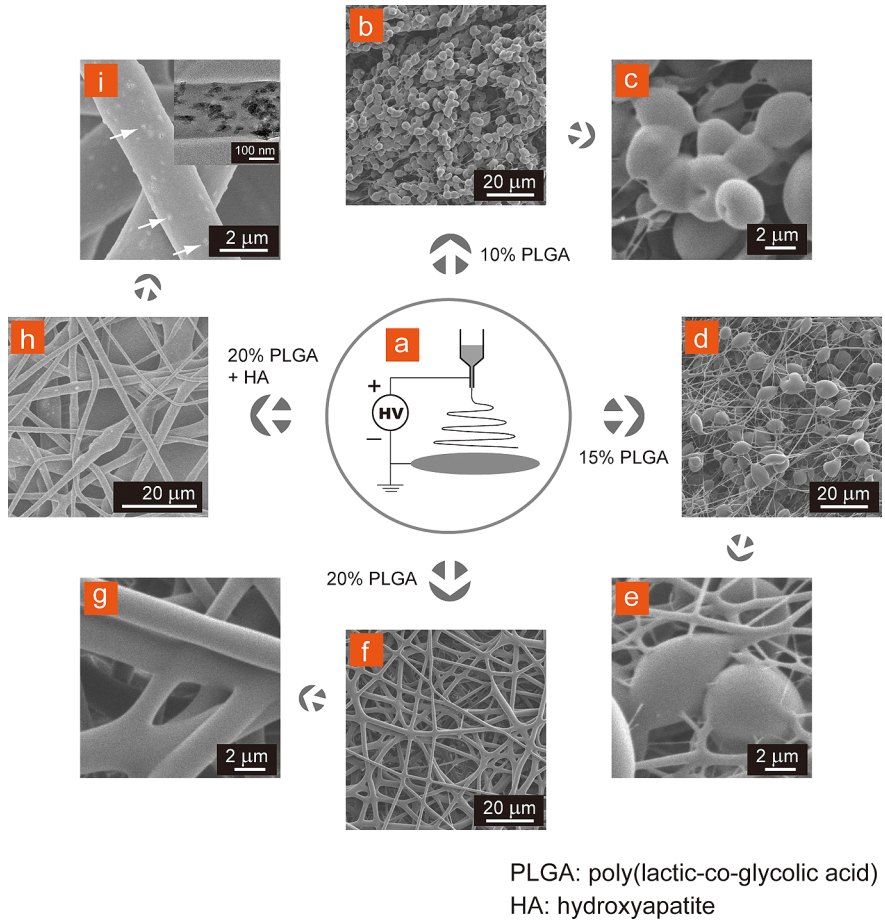

Figure 1. (a) Schematic illustration of ES setup. SEM images of (b) ES poly(lactic-co-glycolic acid) (PLGA) microspheres (10% and 20 kV), (d) beaded fibers (15% and 20 kV), and (f) uniform continuous fibers (20% and 15 kV). (c, e, g) Typical enlarged images of b, d, and f, respectively. (h, i) SEM images of PLGA/nanohydroxyapatite (PLGA/nano-HA) composite fibers. The inset is the TEM image, indicating that nano-HA particles are distributed uniformly inside of fibers. The white arrows in i indicate the nano-HA particles on the surface of ES fibers 304 × 318 mm (150 × 150 DPI).

nonwoven mat. A variety of micro/nanoscale structures, including fibers, tubes, spheres, cups, and even cages, can be fabricated by the ES method.[14−16] Experimental parameters, especially polymer concentration (mainly viscosity) and applied high voltage, are critical for the morphologies of resultant products.[17]

More recently, particular attention has been devoted to fabricate composites of electrospun fibrous scaffolds with both organic polymers and inorganic salts, especially poly(lactic-co-glycolic acid)/hydroxyapatite (PLGA/HA) system, to imitate the organic (collagen)/inorganic (apatites) components of ECM. Jose et al.[18] prepared aligned PLGA/HA nanofibrous scaffolds by ES method, and characterized various experimental parameters on the morphologies of resultant fibers. Moreover, they found that the addition of nano-HA could improve the mechanical properties of the scaffold to some extent. Gao's group[19] prepared similar PLGA nanofibrous scaffolds with embedded bone matrixlike nano-HA particles. The in vitro results revealed that incorporated HA could enhance the biomineralization ability of scaffolds, and improve metabolic activities of MC 3T3 E1 osteoblasts cultured on the composite scaffold. Although substantial efforts have been made to improve the properties of fibrous scaffolds, to date, few studies have employed primary human cells to evaluate the efficacy and biocompatibility of these implantable materials. There is no doubt that the best test species for human is human, and it is impossible to extrapolate the results of animal testing directly to human due to interspecies variation in anatomy, physiology, and biochemistry.[20,21]

Herein, we utilized the ES technique to fabricate PLGA-alone scaffolds with various microstructures, including spheres, beaded fibers, and uniform fibers, and PLGA/nano-HA composite scaffolds. We also evaluated the bone-bonding ability of these materials by examining the formation of apatite on their surfaces in a simulated body fluid. Most importantly, to the best of our knowledge, this is the first report to utilize primary human osteoblasts as a cell model to investigate the performance of electrospun PLGA/nano-HA scaffolds in vitro for human bone repairing.

EXPERIMENTAL SECTION

Materials. Poly(DL-lactide-co-glycolide) (PLGA, 7525 DLG 7E, SurModics) and nanoscale hydroxyapatite (nano-HA, synthesized by ourselves) were used to fabricated electrospun scaffolds with acetone and dimethylformamide as solvents. The simulated body fluid (SBF) solution was prepared as described in ref 23.

Characterization. A scanning electron microscopy (SEM) and a transmission electron microscopy (TEM) were used to observe the morphologies of electrospun scaffolds. A contact angle measuring system was used to test their wetting behaviors, and an inductively

coupled plasma-atomic emission spectrometer (ICP-AES) was used to detect the concentration of Ca^{2+} in SBF.

In Vitro Experiments. With both mouse preosteoblast cell line (MC 3T3 E1) and primary human osteoblasts (HOB) as the cell models, we measured cell viability, alkaline phosphatase (ALP) activity, and osteocalcin concentration to investigate the performance of electrospun scaffolds.

The detailed experimental information is available in Supporting Information.

RESULTS AND DISCUSSION

With different polymer concentrations, we could fabricate various microstructures such as spheres, beaded fibers, and uniform fibers using one-step ES technique.[17] Figure 1a shows the schematic illustration of ES setup we used. By using the ES solution with a PLGA content of 10%, we fabricated the PLGA scaffold with interconnected microspheres of 3.5 ± 0.7 μm in diameter (Figure 1b, c, and Figure S1 in the Supporting Information). As the PLGA concentration increased to 15%, a new fiber morphology appeared, in which bigger microspheres (5.6 ± 1.4 μm in diameter) were connected with each other by micro/nanoscale fibers (Figure 1d, e, and Figure S1 in the Supporting Information). By further increasing the concentration of PLGA to 20%, the polymer solution became more viscous, and the resultant products were the most common microstructures in ES, i.e., uniform superfine fibers with random orientation (Figure 1f, g). Compared with other two scaffolds, the nonwoven mat exhibits the largest pore size (see Figure S1 in the Supporting Information). In all experiments, the working distance was 10 cm, and the operating voltage was 15−20 kV. These experiments show that we can adjust the morphologies of the ES fibers simply by using different concentrations of PLGA.

To further enhance the biocompatibility of PLGA scaffolds and mimic the organic/inorganic nature of ECM, we deposited nanoscale hydroxyapatite (nano-HA), one phase of calcium phosphate and the major inorganic component in bone tissue, into the PLGA scaffolds.[6] For synthesis of nano-HA, we used calcium oxide (CaO) and phosphoric acid (H_3PO_4). Results from the X-ray diffraction (XRD) pattern and TEM images prove that our synthesized powder contain nano-HA particles with dimensions of 205 ± 40 nm in length, 33 ± 6 nm in width, and 6 ± 1 in length/width ratio (see Figure S2 in the Supporting Information). To disperse nano-HA particles, we injected nano-HA solution into transparent 20% PLGA solution drop by drop for several times with constant stirring and ultrasonication. After treatment, the final solution became a white suspension which was immediately used for electrospinning. We can observe nano-HA particles on the surface of ES composite fibers from SEM image, which are indicated by white arrows in Figure 1i. The TEM image demonstrates that nano-HA particles are distributed uniformly in ES fibers (inset in Figure 1i). In this work, the weight ratio of nano-HA and PLGA in composite fibers is 3:7 which might be the highest weight ratio in electrospun PLGA/nano-HA fibers to sustain the stability.

After obtaining three types of PLGA mats with different topographies and one PLGA/nano-HA mat, we characterized their wettability and bone-bonding ability.[22,23] Contact angle measurements showed that all of these PLGA samples were hydrophobic with nearly the same contact angle values, regardless of their microstructures such as microspheres, beaded fibers, and uniform fibers (136.7 ± 0.5, 138.2 ± 2.1, and 136.8 ± 0.7, respectively). However, the contact angle value of PLGA/nano-HA composite scaffold decreased slightly in comparison with PLGA-alone scaffold, revealing that nano-HA can enhance the hydrophility of scaffold (see Table S1 in the Supporting Information).[26]

Moreover, the bone-bonding ability of PLGA-alone and PLGA/nano-HA scaffolds was evaluated by examining the formation of apatite on scaffold surface in a simulated body fluid (SBF) with ion concentrations similar to those of human blood plasma.[23] For three PLGA-alone scaffolds with different microstructures into SBF for 3 weeks, a small amount of bonelike apatites formed on the surfaces and appeared as discrete dots (Figure 2a−c). In addition, the morphologies of PLGA-alone scaffolds changed such that the microstructures stuck together and the space among them became smaller. This could be attributed to the slight degradation of PLGA during incubation in an aqueous environment (see Figure S3 in the Supporting Information). For PLGA/nano-HA scaffolds, only a few apatites were formed in the first 4 days. However, with the increased incubation time to 7 days, more apatites were crystallized and observed. After 3 week incubation in SBF solution, PLGA/nano-HA fibers were covered totally with a large quantity of apatites and their diameters increased dramatically to approximately 7 μm, an increase of 3 times (Figure 2d), which is completely different from the phenomenon on the surfaces of PLGA-alone mats, where the diameter of the fibers barely changed (see Figure S3 in the Supporting Information). This low degradation of PLGA fibers is consistent with the reported results[24] and the information provided by the manufacturer.[25] These results verify that nano-HA in composite scaffold could greatly enhance the formation of bonelike apatites.

To quantitatively evaluate calcium phosphate formation on sample surface, we plotted Ca^{2+} concentration in SBF solution as a function of incubation time in Figure 2e. After incubation for 1 day, $[Ca^{2+}]$ in SBF solution decreased from 100 μg/mL (original concentration, 25 mM[23]) to around 85 μg/mL for all samples (including three PLGA-alone samples with different surface structures and one PLGA/nano-HA composite sample). For three PLGA-alone samples, $[Ca^{2+}]$ oscillated in the range between 80 and 85 μg/mL during the 21 day incubation. For PLGA/nano-HA scaffolds, we found that $[Ca^{2+}]$ in the solution decreased linearly as the incubation time increased (Figure 2f). Meanwhile, crystals of bonelike apatites were formed on the ES fibers (the inset in Figure 2f). At the 21st day, the remaining $[Ca^{2+}]$ was below 55 μg/mL, indicating a consumption of approximately 45% of calcium ions. This value was three times higher than that of PLGA-alone samples.

During the process of incubation in SBF at 36.5 °C, all PLGA-alone and PLGA/nano-HA mats shrank to some extent, as shown in Figure 2g. Herein, the shrinkage is defined as $(S_0 - S)/S_0$, where S_0 is the original area of mat, and S is the measured area after incubation. We observed that most shrinkage of the mats' area occurred in the first 24 h, and almost halted in the next 3 weeks. This shrinkage might be due to the recoiling effect of electrospun fibers after incubation in the medium.[18] Among six repeats of three types of PLGA-alone mats with different morphologies, the highest shrinkage of 80% was from microspheres that were fabricated by electrospinning 10% PLGA solution, and the lowest of approximately 60% was from uniform fibers which were electrospun using 20% PLGA solution. Therefore, to minimize shrinkage, it is necessary to electrospin PLGA into uniform fibers. In comparison, PLGA/nano-HA composite scaffold had a smaller shrinkage (less than

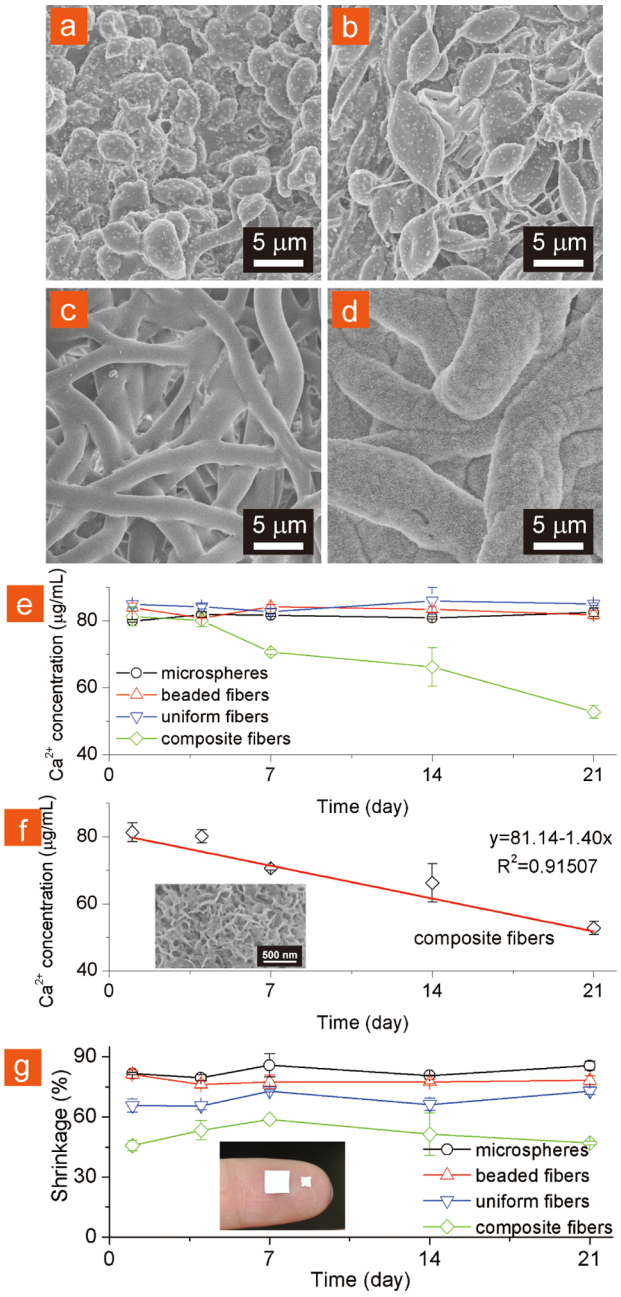

Figure 2. SEM images of different ES mats after incubation in SBF for 21 days: (a) microspheres, (b) beaded fibers, (c) uniform fibers, and (d) PLGA/nano-HA fibers. (e) Relationships between Ca^{2+} concentration in SBF and time after ES mats were incubated with the SBF. (f) Ca^{2+} concentration versus time for composite fibers. The inset is the SEM image of hydroxyaptite formed in SBF. (g) Shrinkage of four types of ES mats after being incubated into SBF solutions for 1, 4, 7, 14, and 21 days. The inset is a digital image of an original ES mat and the one incubated in SBF on a finger. Shrinkage = $(S - S_0)/S_0$, where S_0 is the original area of mat, and S is the area after incubated into SBF. Data produced from six repeats. 168 × 293 mm (150 × 150 DPI).

50%) than PLGA-alone samples (60−80%). On the basis of these results, we consider that the embedded nano-HA particles inside the PLGA/nano-HA scaffold can impede the chain mobility of PLGA and inhibit the dissolution of PLGA, thus reducing the shrinkage of scaffold.

The above studies suggest that electrospun PLGA/nano-HA scaffold has a better bone-bonding ability and antishrinkage performance than PLGA-alone scaffolds. To test biocompatibility of these scaffolds, we cultured mouse preosteoblast cell line (MC 3T3 E1) on the surfaces of PLGA-alone and PLGA/nano-HA scaffolds in vitro. Four ES scaffolds, including microspheres, beaded fibers, uniform fibers, and composite fibers, were cut into small pieces (1 cm × 1 cm). After sterilization, MC 3T3 E1 cells were seeded and cultured on ES scaffolds. Figure 3a reveals that MC 3T3 E1 cells grew rapidly

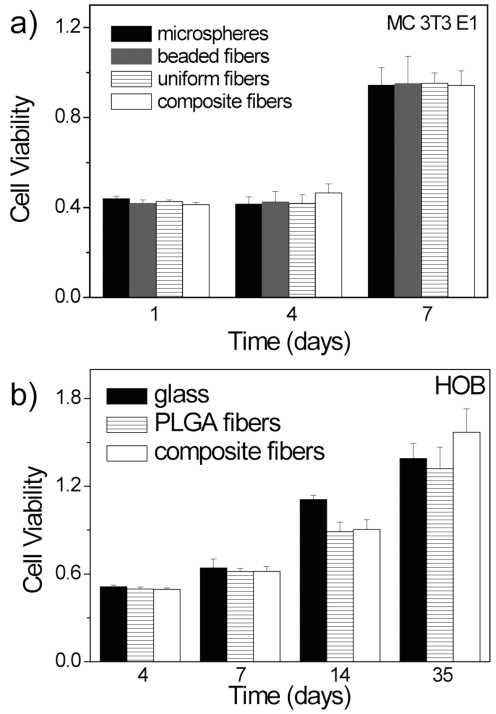

Figure 3. Bioactivity of (a) MC 3T3 E1 (7 days) and (b) HOB cells (35 days) cultured on different types of ES PLGA mats. 134 mm × 194 mm (150 × 150 DPI).

on all scaffolds, and there is no significant difference in cell viability among four scaffolds during a period of 7 days, which is consistent with the published results.[19] This result implies that both the microscale structure and nano-HA have minor effects on viability of MC 3T3 E1 osteoblasts cultured on PLGA scaffolds. Furthermore, the morphology of cells attached on scaffolds was inspected using a Zeiss LSM 710 confocal microscope after 1 week of culturing. Confocal fluorescent microscopic images show that cells on PLGA/nano-HA composite fibers had more pseudopodia and spread better than PLGA-alone scaffolds (see Figure S4 in the Supporting Information). This is expected because of the enhanced mineralization and osteogenesis induced by nano-HA.[27] Long-term culture of MC 3T3 E1 osteoblasts was not carried out because cells covered the entire surface of scaffolds at day 7. The previous literature also indicated that both the cell viability and proliferation decayed with prolonged culture time because of the contact inhibition effect at the large cell number.[19]

Next we isolated primary human osteoblasts (HOB), and employed this type of cells to test performances of PLGA uniform fibers and PLGA/nano-HA fibers. Glass slides with the same area were used as control. The in vitro results are exhibited in Figure 3b. In the first week, all samples including

dx.doi.org/10.1021/am401937m | ACS Appl. Mater. Interfaces 2013, 5, 5921−5926

control nearly had the same cell viability value. In the second week, there was a slight difference in cell viability for two ES scaffolds, whereas cells cultured on the control showed faster proliferation. This is because osteoblasts like to attach to two-dimensional flat substrates such as glass and Petri dish during the first few days after seeding.[28] It is also noteworthy that HOB on composite scaffold spread better than PLGA scaffold and glass substrate, similar with the observation of MC 3T3 E1 cells (Figure 4). Meanwhile, confocal images indicate that HOB

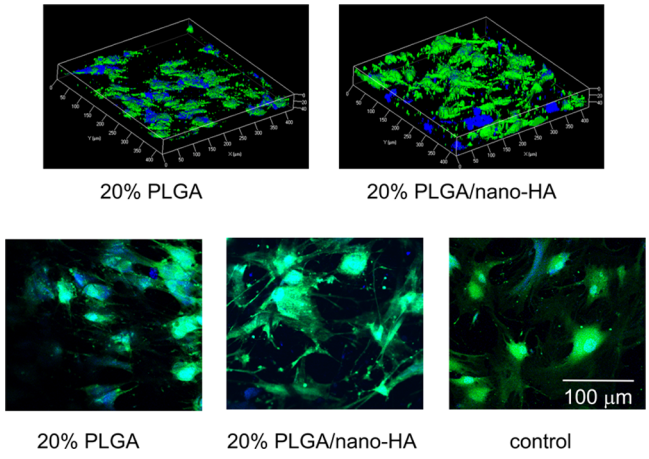

Figure 4. Confocal fluorescent microscopic images of HOB cells cultured on 20% PLGA mat, 20% PLGA/nano-HA mat, and glass after 14 days. The three bottom images share the same scale bar. HOB cells were stained with Hoechst (blue) and 3099 (green). 150 mm × 106 mm (150 × 150 DPI).

cells on PLGA/nano-HA scaffold were connected with each other by visible pseudopodia. After 2 weeks, the growth rate of HOB cultured on the control substrate decreased dramatically. Meanwhile, the cell proliferation rate on PLGA fibers was slightly faster. Nevertheless, the growth rate of HOB on the composite scaffold kept a higher increase, which may be due to the presence of nano-HA. By the last week (the fifth week), the number of viable cells was the highest in the composite scaffold among all three types of samples, which may result from the following two reasons. First, ES composite scaffold with porous/fibrous microstructures is suitable for cell adhesion which was confirmed by confocal observation of HOB cells (Figure 4). Second, the deposited nano-HA may promote the proliferation of HOB cells. Figure 3b provides more detailed comparisons of HOB cell viability in the last week. It can be clearly seen that the cell viability of composite fibers was 18.9% and 12.9% higher than that of PLGA fibers and control separately. All these results suggest that the three-dimensional electrospun PLGA/nano-HA scaffolds may serve as a potential candidate in human bone repair.

In addition, to evaluate the differentiation behavior of MC 3T3 E1 and HOB cultured on electrospun scaffolds, we performed the measurements of alkaline phosphatase (ALP, the early marker for osteoblastic differentiation) activity and osteocalcin concentration secreted in culture medium (later marker related to bone biomineralization).[29] When using MC 3T3 E1 as the cell model, both the ALP activity and osteocalcin concentration were not significantly different between PLGA-alone and PLGA/nano-HA scaffolds (see Figures S5 and S6 in the Supporting Information, the increase is only 3% and 1% separately). However, during 2 weeks of HOB culturing, we found that PLGA/nano-HA composite scaffold could prompt ALP activity (~9%) and increase osteocalcin concentration (~16%) in comparison with PLGA-alone scaffold (see Figures S5 and S6 in the Supporting Information). These results are consistent with the cell viability in Figure 3, suggesting that PLGA/nano-HA scaffold is a good candidate in human bone tissue engineering. Moreover, the use of HOB to test the performance of scaffolds instead of cell lines such as MC 3T3 E1 may yield a higher clinical significance.

CONCLUSION

In summary, the PLGA-alone fibrous scaffolds with different microscale morphologies and the PLGA/nano-HA composite scaffold were prepared by ES approach. The microscale morphologies fabricated by electrospinning solutions with different concentrations have slightly influence on biomineralization. In comparison, the embedded nano-HA can significantly enhance the formation of the bone-like apatites. Moreover, we adopted both primary human osteoblast and MC 3T3 E1 as model cells to evaluate the performance of PLGA-alone and PLGA/nano-HA scaffolds. In vitro experiments including cell viability, ALP activity, and osteocalcin concentration demonstrate that PLGA/nano-HA composite scaffold can promote the response of HOB better than MC 3T3 E1, thus showing great promise for human bone repair.

ASSOCIATED CONTENT

Supporting Information

Experimental details and additional figures (PDF). This material is available free of charge via the Internet at http://pubs.acs.org.

AUTHOR INFORMATION

Corresponding Author

*E-mail: xingyujiang@nanoctr.cn (X.J.); sunjs@nanoctr.cn (J.S.); yunze.long@163.com (Y.-Z.L.).

Author Contributions

§Authors M.L. and W.L. contributed equally to this work

Notes

The authors declare no competing financial interest.

ACKNOWLEDGMENTS

Prof. Xingyu Jiang acknowledges the financial support of MOST (2009CB930001, 2011CB933201, and 2012AA030308), NSFC (21025520, 21025520, 51105086, and 51073045), and CAS (KJCX2-YW-M15). Prof. Yun-Ze Long acknowledges the financial support of the National Natural Science Foundation of China (11074138), the Shandong Provincial Natural Science Foundation for Distinguished Young Scholars (JQ201103), the Taishan Scholars Program of Shandong Province, China, and the National Key Basic Research Development Program of China (973 special preliminary study plan, 2012CB722705). The authors thank Dr. Zhijie Yang for valuable discussions.

REFERENCES

(1) Murugan, R.; Ramakrishna, S. *Compos. Sci. Technol.* **2005**, *65*, 2385.
(2) Zheng, W.; Zhang, W.; Jiang, X. *Adv. Eng. Mater.* **2010**, *12*, B451.
(3) Beachley, V.; Wen, X. *Prog. Polym. Sci.* **2010**, *35*, 868.
(4) Newcomb, C. J.; Bitton, R.; Velichko, Y. S.; Snead, M. L.; Stupp, S. I. *Small* **2012**, *8*, 2195.

(5) MaHam, A.; Tang, Z.; Wu, H.; Wang, J.; Lin, Y. *Small* **2009**, *5*, 1706.
(6) Stevens, M. M.; George, J. H. *Science* **2005**, *310*, 1135.
(7) (a) Li, M.; Long, Y.-Z.; Yang, D.; Sun, J.; Yin, H.; Zhao, Z.; Kong, W.; Jiang, X.; Fan, Z. *J. Mater. Chem.* **2011**, *21*, 13159. (b) Zoppe, J. O.; Peresin, M. S.; Habibi, Y.; Venditti, R. A.; Rojas, O. J. *ACS Appl. Mater. Interfaces* **2009**, *1* (9), 1996.
(8) Yuan, B.; Jin, Y.; Sun, Y.; Wang, D.; Sun, J.; Wang, Z.; Zhang, W.; Jiang, X. *Adv. Mater.* **2012**, *24*, 890.
(9) Hartgerink, J. D.; Beniash, E.; Stupp, S. I. *Science* **2001**, *294*, 1684.
(10) Grimm, S.; Giesa, R.; Sklarek, K.; Langner, A.; Gösele, U.; Schmidt, H.-W.; Steinhart, M. *Nano Lett.* **2008**, *8*, 1954.
(11) (a) Rollings, D.-a. E.; Tsoi, S.; Sit, J. C.; Veinot, J. G. C. *Langmuir* **2007**, *23*, 5275. (b) Rodriguez, K.; Renneckar, S.; Gatenholm, P. *ACS Appl. Mater. Interfaces* **2011**, *3* (3), 681.
(12) Jang, J.; Chang, M.; Yoon, H. *Adv. Mater.* **2005**, *17*, 1616.
(13) Yang, D. Y.; Lu, B.; Zhao, Y.; Jiang, X. Y. *Adv. Mater.* **2007**, *19*, 3702.
(14) (a) Long, Y.-Z.; Li, M.-M.; Gu, C.; Wan, M.; Duvail, J.-L.; Liu, Z.; Fan, Z. *Prog. Polym. Sci.* **2011**, *36*, 1415. (b) Li, M.; Yang, D.; Long, Y.; Ma, H. *Nanoscale* **2010**, *2*, 218.
(15) (a) Mattanavee, W.; Suwantong, O.; Puthong, S.; Bunaprasert, T.; Hoven, V. P.; Supaphol, P. *ACS Appl. Mater. Interfaces* **2009**, *1* (5), 1076. (b) Ifkovits, J. L.; Devlin, J. J.; Eng, G.; Martens, T. P.; Vunjak-Novakovic, G.; Burdick, J. A. *ACS Appl. Mater. Interfaces* **2009**, *1* (9), 1878. (c) Dinarvand, P.; Seyedjafari, E.; Shafiee, A.; Babaei Jandaghi, A.; Doostmohammadi, A.; Fathi, M. H.; Farhadian, S.; Soleimani, M. *ACS Appl. Mater. Interfaces* **2011**, *3* (11), 4518.
(16) Zhao, Y.; Cao, X. Y.; Jiang, L. *J. Am. Chem. Soc.* **2007**, *129*, 764.
(17) Lu, X.; Wang, C.; Wei, Y. *Small* **2009**, *5*, 2349.
(18) Jose, M. V.; Thomas, V.; Johnson, K. T.; Dean, D. R.; Nyairo, E. *Acta Biomater.* **2009**, *5*, 305.
(19) Lao, L.; Wang, Y.; Zhu, Y.; Zhang, Y.; Gao, C. *J. Mater. Sci.—Mater. Med.* **2011**, *22*, 1873.
(20) MacLennan, A. *Cosmetics and Toiletries Manufacturers and Suppliers*; Clinical Science Research Ltd.: UK, 1990; Vol. *XVII*, p 24.
(21) Leung, W. K.; Bjarnason, I.; Chan, F. K. L. *The Lancet* **2007**, *369*, 1691.
(22) Feng, X. J.; Jiang, L. *Adv. Mater.* **2006**, *18*, 3063.
(23) Kokubo, T.; Takadama, H. *Biomaterials* **2006**, *27*, 2907.
(24) Fouad, H.; Elsarnagawy, T.; Almajhdi, F. N.; Khalil, K. A. *Int. J. Electrochem. Sci.* **2013**, *8*, 2293.
(25) Evonik Industries Home Page. http://biomaterials.evonik.com (accessed Jun 18, 2013).
(26) Tihan, T. G.; Ionita, M. D.; Popescu, R. G.; Iordachescu, D. *Mater. Chem. Phys.* **2009**, *118*, 265.
(27) Zhang, P.; Hong, Z.; Yu, T.; Chen, X.; Jing, X. *Biomaterials* **2009**, *30*, 58.
(28) Nie, H.; Soh, B. W.; Fu, Y.-C.; Wang, C.-H. *Biotechnol. Bioeng.* **2008**, *99*, 223.
(29) Horii, A.; Wang, X.; Gelain, F.; Zhang, S. *PloS one* **2007**, *2*, e190.